

Aberystwyth University

*High-resolution genetic analysis reveals extensive gene flow within the jellyfish *Pelagia noctiluca* (Scyphozoa) in the North Atlantic and Mediterranean Sea*

Glynn, Fergal; Houghton, Jonathan D. R.; Bastian, Thomas; Doyle, Thomas K.; Fuentes, Veronica; Lilley, Martin K. S.; Provan, Jim

Published in:

Biological Journal of the Linnean Society

DOI:

[10.1111/bij.12654](https://doi.org/10.1111/bij.12654)

Publication date:

2016

Citation for published version (APA):

Glynn, F., Houghton, J. D. R., Bastian, T., Doyle, T. K., Fuentes, V., Lilley, M. K. S., & Provan, J. (2016). High-resolution genetic analysis reveals extensive gene flow within the jellyfish *Pelagia noctiluca* (Scyphozoa) in the North Atlantic and Mediterranean Sea. *Biological Journal of the Linnean Society*, 117(2), 252-263.
<https://doi.org/10.1111/bij.12654>

General rights

Copyright and moral rights for the publications made accessible in the Aberystwyth Research Portal (the Institutional Repository) are retained by the authors and/or other copyright owners and it is a condition of accessing publications that users recognise and abide by the legal requirements associated with these rights.

- Users may download and print one copy of any publication from the Aberystwyth Research Portal for the purpose of private study or research.
- You may not further distribute the material or use it for any profit-making activity or commercial gain
- You may freely distribute the URL identifying the publication in the Aberystwyth Research Portal

Take down policy

If you believe that this document breaches copyright please contact us providing details, and we will remove access to the work immediately and investigate your claim.

tel: +44 1970 62 2400

email: is@aber.ac.uk

High-resolution genetic analysis reveals extensive gene flow within the jellyfish *Pelagia noctiluca* (Scyphozoa) in the North Atlantic and Mediterranean Sea

FERGAL GLYNN^{1,2}, JONATHAN D. R. HOUGHTON^{1,2,3}, THOMAS BASTIAN⁴,
THOMAS K. DOYLE⁵, VERÓNICA FUENTES⁶, MARTIN K. S. LILLEY⁷
and JIM PROVAN^{1,2*}

¹ *School of Biological Sciences, Queen's University Belfast, 97 Lisburn Road, Belfast BT9 7BL, UK*

² *Institute for Global Food Security, Queen's University Belfast*

³ *Queen's Marine Laboratory, 12-13 The Strand, Portaferry, BT22 1PF, UK*

⁴ *Université du Littoral Côte d'Opale, L.O.G. UMR-8187, M.R.E.N. 32 av. du Maréchal Foch, F-62930 Wimereux, France*

⁵ *Zoology, School of Natural Sciences, Ryan Institute, National University of Ireland Galway, Galway, Ireland*

⁶ *Marine Science Institute, Spanish National Research Council, Barcelona, Spain*

⁷ *School of Biological and Chemical Sciences, Queen Mary University of London, Mile End, E1 4NS, UK*

*Corresponding author: Dr Jim Provan

E-mail: J.Provan@qub.ac.uk

Tel: +44 (0)28 9097 2280

Fax: +44 (0)28 9097 5588

1 Despite the importance of gelatinous zooplankton as components of marine ecosystems, both
2 ecologically and socio-economically, relatively little is known about population persistence
3 or connectivity in jellyfish. In the present study, we employed a combination of nuclear
4 microsatellite markers and sequence data from the mitochondrial cytochrome oxidase I (COI)
5 gene to determine levels and patterns of population genetic structuring in the holoplanktonic
6 jellyfish *Pelagia noctiluca* across the northeast Atlantic Ocean and Mediterranean Sea. Our
7 results indicate a high degree of connectivity in *P. noctiluca*, with little evidence of
8 geographical structuring of genetic variation. A small but significant differentiation of
9 Atlantic Ocean and Mediterranean stocks was detected based on the microsatellite data, but
10 no evidence of differentiation was observed with the mtDNA, probably due to the higher
11 power of the microsatellites to detect low levels of genetic structuring. Two clearly distinct
12 groups of genotypes were observed within the mtDNA COI, which probably diverged in the
13 early Pleistocene, but with no evidence of geographical structuring. Palaeodistribution
14 modelling of *P. noctiluca* at the Last Glacial Maximum (LGM; *ca.* 21 KYA) indicated large
15 areas of suitable habitat south of the species' current-day distribution, with little reduction in
16 area. The congruent evidence for minimal genetic differentiation from the nuclear
17 microsatellites and the mtDNA, coupled with the results of the palaeodistribution modelling,
18 supports the idea of long-term population stability and connectivity, thus providing key
19 insights into the population dynamics and demography of this important species.

20
21 **ADDITIONAL KEYWORDS:** Gelatinous zooplankton, jellyfish, microsatellites,
22 mitochondrial COI, palaeodistribution modelling, *Pelagia noctiluca*, population genetics

INTRODUCTION

Jellyfish (i.e. Phylum Cnidaria, Class Scyphozoa) exhibit a range of life history strategies. Most are metagenic, with an asexually reproducing, life-stage which is benthic (the polyp) and a free swimming or planktonic life stage (the medusa) among other, intermediate, stages (Arai, 1997). Such species are often constrained spatially by the need for accessible substratum for the settlement of polyps, skewing the distribution of resultant blooms towards near-shore waters (Boero *et al.*, 2008). In turn, metagenic jellyfish tend to exhibit population structure at modest scales (e.g. Lee *et al.*, 2013), predictable geographical distribution (e.g. Houghton *et al.*, 2006a) and relatively predictable, seasonal blooms (e.g. Houghton *et al.*, 2006b). Some jellyfish species, however, lack this benthic life stage enabling individuals to reproduce more readily in deeper off-shore waters (Boero *et al.*, 2008). *Pelagia noctiluca* is one such species with an apparently vast geographical range spanning the Atlantic, Pacific and Indian Oceans as well as their adjacent seas (Kramp, 1961; Mariottini, Giacco & Pane, 2008). Unlike blooms of metagenic jellyfish which arise from asexual strobilation at the seabed, the free-swimming medusae of *P. noctiluca* arise solely from sexual reproduction in the water column (Rottini Sandrini & Avian, 1983) which may convey a competitive advantage in deep-water habitats. At times, they can be brought onto continental shelves by oceanic water overflow, as is the case on the Irish Continental Shelf (Fraser, 1956; Bastian *et al.*, 2011). Indeed, in this region the species has been known to form aggregations $> 4^{\circ}$ of latitude (Doyle *et al.*, 2008) and to strand along hundreds of kilometres of coastline numerous times in recent years (Fleming, Harrod & Houghton, 2013).

Understanding the population connectivity of jellyfish has relevance far beyond the prediction of socio-economic impacts (Doyle *et al.*, 2014) with Pauly *et al.* (2008) describing them as ‘arguably the most important predators or the sea’. As one of the most venomous

species in UK/Irish waters (Mariottini *et al.*, 2008), *P. noctiluca* is certainly a noteworthy predator yet, like many gelatinous species, is given scant consideration in fisheries or ecosystem models (Pauly *et al.*, 2008; Sabates *et al.*, 2010; Doyle *et al.*, 2014; Purcell *et al.*, 2014). On a regional scale, the species first gained notoriety in the Northeast Atlantic following a major fish kill at salmon farms in Northern Ireland in November 2007 causing >£1M in damages in a single day (Doyle *et al.*, 2008). At first this mass incursion of this species in Irish/UK coastal waters in 2007 was reported as unprecedented, yet subsequent desktop studies revealed that *P. noctiluca* was reported in Irish/UK waters in 21 out of a possible 95 years (i.e. 1890-1985; Doyle *et al.*, 2014). More recent studies using beach strandings (Fleming *et al.*, 2013), fisheries by-catch data (Bastian *et al.*, 2011) and continuous plankton recorder records (Licandro *et al.*, 2010) have confirmed that the species is a longstanding feature of Irish/UK shelf waters. Given the ecological implications of these reoccurring blooms (Doyle *et al.*, 2014) and the economic threat they pose to the Irish/UK aquaculture industry (Doyle *et al.*, 2008; Fleming, Harrod & Houghton, 2013) there is a pressing need to understand the demographic processes that underpin them better.

Within this context, molecular genetics provides the opportunity to explore patterns of connectivity and recruitment underpinning blooms of *P. noctiluca*. Such concepts are pertinent following Licandro *et al.* (2010), who suggested that the prevalence of *P. noctiluca* in the northeast Atlantic (NEA) during 2007 and 2008 may reflect recent hydrographic changes in the region. More specifically, the authors suggested that outbreaks of *P. noctiluca* may follow the progression of the North Atlantic Current (NAC) and the continental slope current (CSC), a northward branch of the Azores Current that flows along the eastern slope boundary of the European basin (Garcia-Soto *et al.*, 2002; Pingree, 2002). It was Fraser (1955) who first proposed that a subsurface current carries the “Lusitanian fauna” from the

outflow of the Gulf of Gibraltar to the NEA. The Lusitanian fauna contains zooplankton species more typically of the Mediterranean, such as *P. noctiluca*.

From a molecular perspective most studies of population structure in *P. noctiluca* to date, and indeed jellyfish in general (reviewed in Glynn, Houghton & Provan, 2015), have relied heavily on the mitochondrial cytochrome oxidase I (COI) gene, occasionally with the addition of ribosomal markers such as the internal transcribed spacers ITS1 and ITS2 (e.g. Stopar *et al.*, 2010). While variable, the uniparental mode of inheritance and small effective population size of the mitochondrial genome (relative to that of the nuclear genome) means that the COI may not be an ideal candidate marker for such studies, particularly where levels of genetic structuring are low. Indeed, previous studies have provided somewhat conflicting findings with respect to connectivity in *P. noctiluca*. Using a combination of COI and ITS, Stopar *et al.* (2010) observed a lack of genetic or geographic structuring across the Eastern Atlantic and Mediterranean Sea whilst Miller, von der Heyden & Gibbons (2012) proposed significant structuring between North and South Atlantic populations.

The application of high-resolution microsatellite markers has been effective in uncovering cryptic population structure across the ranges of several marine species that had been thought previously to be panmictic, such as eels (Wirth & Bernatchez, 2001) and microalgae (Provan, 2010). The sole population genetics of *P. noctiluca* to date that employed multiple, unlinked, microsatellite markers focused on smaller-scale population structuring within the Eastern Mediterranean and the Adriatic Seas (Agieri *et al.*, 2014). Consequently, in the present study we employed the same microsatellites to analyse large-scale patterns of variation over a similar area studied by Stopar *et al.* (2010), but with more extensive sampling of the Northeast Atlantic, since population structuring as a result of historical processes have been documented in the region for several marine species (reviewed in Provan, 2013). We wanted to determine whether there was any significant differentiation between *P. noctiluca* from the

97 North Atlantic and populations from the Mediterranean Sea following the suggestions of
98 Licandro *et al.* (2010), the historical observation of Fraser (1955), and given that the Strait of
99 Gibraltar has been proposed to be a biogeographic barrier (reviewed in Patarnello, Volckaert
100 & Castilho, 2007), and also whether there was any finer-scale structuring within regions.

MATERIALS AND METHODS

SAMPLING AND DNA EXTRACTION

Samples were obtained from live-caught or fresh shore-stranded aggregations of *P. noctiluca* (locations are listed in Table 1). Specimens were washed in sea water before whole individuals in some cases, or umbrellar/gonadal flesh samples in most cases, were preserved in ethanol. All samples were stored in a 1:3 flesh to ethanol ratio, then stored at -20°C until extraction. Immediately prior to extraction, flesh was removed from the ethanol and dried using sterile paper towels, rinsed in double-distilled water and dried again on sterile paper towels to remove traces of ethanol. Genomic DNA was extracted using a modified version of the Porebski, Bailey & Baum (1997) CTAB phenol/chloroform protocol whereby extracted DNA which had been subjected to phenol and chloroform wash was stored in a 1:1 supernatant:isopropanol state at -20°C until needed for PCR, then pelleting and the alcohol wash were carried out before elution. Long term storage of eluted DNA resulted in loss of high molecular weight (genomic) DNA and reduced amplification success.

MICROSATELLITE GENOTYPING

We utilised eight of the nine microsatellite loci reported for *P. noctiluca* by Aglieri *et al.* (2014), with the exception of locus Pelnoc_40199, which could not be consistently amplified. Forward primers included a 19 bp M13 tail (CACGACGTTGTAAAACGAC) and reverse primers included a 7 bp tail (GTGTCTT). PCR was carried out in a total volume of 10 µl containing 100 ng genomic DNA, 10 pmol of 6-FAM-, PET- or HEX-labelled M13 primer, 1 pmol of tailed forward primer, 10 pmol reverse primer, 1x PCR reaction buffer, 200 µM each dNTP, 2.5 mM MgCl₂ and 0.25 U GoTaq Flexi DNA polymerase (Promega). PCR was carried out on a MWG Primus thermal cycler using the following parameters: initial

denaturation at 94 °C for 5 min followed by 45 cycles of denaturation at 94 °C for 30 s, annealing at 57 °C for 30 s, extension at 72 °C for 30 s and a final extension at 72 °C for 5 min. Genotyping was carried out on an AB3730xl capillary genotyping system (Life Technologies; Carlsbad, California, USA). Allele sizes were scored using LIZ size standards and were checked by comparison with previously sized control samples.

MTDNA SEQUENCING

A 532 bp region of the *P. noctiluca* mtDNA COI gene was amplified using the primers Pn-COI-F 5'-CCAGGGTCAATGCTTGGAG-3' and Pn-COI-R 5'-CGAAGAAAGAGGTGTTAAAGTT-3' designed from GenBank sequence GQ376003. PCR was carried out on a MWG Primus thermal cycler using the following parameters: initial denaturation at 94 °C for 3 min followed by 45 cycles of denaturation at 94 °C for 30 s, annealing at 58 °C for 30 s, extension at 72 °C for 1 min and a final extension at 72 °C for 5 min. PCR was carried out in a total volume of 20 µl containing 200 ng genomic DNA, 10 pmol of each primer, 1x PCR reaction buffer, 200 µM each dNTP, 2.5 mM MgCl₂ and 0.5 U GoTaq Flexi DNA polymerase (Promega). 5 µl PCR product were resolved on 1.5% agarose gels and visualised by ethidium bromide staining, and the remaining 15 µl were EXO-SAP purified and sequenced in both directions using the BigDye sequencing kit (V3.1; Applied Biosystems) and run on an AB 3730XL DNA analyser (Life Technologies; Carlsbad, California, USA).

DATA ANALYSIS

Tests for linkage disequilibrium between pairs of microsatellite loci in each population were carried out in the program FSTAT (V2.9.3.2; Goudet, 2002). Levels of polymorphism measured as observed (H_O) and expected (H_E) heterozygosity averaged over loci for nuclear

microsatellites, and as haplotype (H) and nucleotide (π) diversity for mtDNA, were calculated using the ARLEQUIN software package (V3.5.1.2; Excoffier & Lischer, 2010). Inbreeding coefficients (F_{IS}) were estimated using FSTAT. To determine the mean levels of relatedness between sampled individuals within populations, the relatedness coefficient (r) of Queller & Goodnight (1989) was calculated using the GENALEX software package (V6.1; Peakall & Smouse, 2006), and significance calculated using 999 permutations.

Levels of overall interpopulation differentiation as well as differentiation between Atlantic and Mediterranean populations and population-pairwise differentiation were estimated from allele (microsatellite) and haplotype (mtDNA) frequencies using Φ -statistics, which give an analogue of F -statistics (Weir & Cockerham, 1985) calculated within the analysis of molecular variance (AMOVA) framework (Excoffier, Smouse & Quattro, 1992), also using the ARLEQUIN software package. A median-joining network showing the relationships between the mtDNA haplotypes was constructed using the NETWORK software package (V4.5.1.6; www.fluxus-engineering.com). The divergence time (T) between the two observed groups of mtDNA haplotypes was estimated by calculating Nei's genetic distance (D_A) using the DNAsp software package (Librado & Rozas, 2009), and by using the formula $T = D_A / 2\mu$ (Nei & Kumar, 2000), where μ , the mutation rate per site per year, was 6.54×10^{-9} , the rate estimated previously for the Cnidarian *Obelia geniculata* (Govindarajan, Halanych & Cunningham, 2005). In addition, tests for population expansion based on Tajima's D and Fu and Li's F and a mismatch distribution analysis, which identifies characteristic "waves" in the shape of the distribution resulting from expansion (Rogers and Harpending, 1992), were carried out for both the large and the small clades in DNAsp.

To identify possible spatial patterns of gene flow, the software package BAPS (V5; Corander, Waldmann & Sillanpää, 2003) was used to identify clusters of genetically similar populations using a Bayesian approach. Ten replicates were run for all possible values of the

maximum number of clusters (K) up to $K = 14$, the number of populations sampled in the study, with a burn-in period of 10 000 iterations followed by 50 000 iterations. Multiple independent runs always gave the same outcome. To further identify possible spatial patterns of gene flow, a principal coordinate analysis (PCA) was carried out in GENALEX. Inter-individual genetic distances were calculated as described in Smouse & Peakall (1999), and the PCA was carried out using the standard covariance approach.

Because of the genetic homogeneity revealed by the microsatellite loci studied, and to compare the relative power of microsatellites and the mtDNA to detect low levels of population differentiation, simulations were carried out using the POWSIM software package (V4.0; Ryman & Palm, 2006). Simulations were carried out for an effective population size of $N_e = 1\,000$ to yield F_{ST} values of 0.001 – 0.020. In all cases, 1 000 replicates were run and the power of the analysis was indicated by the proportion of tests that were significant at $P < 0.05$ using the observed allele frequencies for both the four microsatellite loci and the single mtDNA COI region studied (for $F_{ST} = 0$ this corresponds to the Type I [α] error). For the mtDNA, sample sizes were adjusted as recommended by Larsson *et al.*, (2009).

PALAEODISTRIBUTION MODELLING

Palaeodistribution modelling was carried out to determine the potential suitable range for *P. noctiluca* at the Last Glacial Maximum (LGM; *ca.* 21 KYA) using the maximum entropy approach implemented in the MAXENT software package (V3.3.3; Phillips, Anderson & Schapire, 2006). Species occurrence data between 1950 and 2000 were downloaded from the Global Biodiversity Information Facility data portal (www.gbif.org) and from the Ocean Biogeographic Information System (www.iobis.org), and supplemented with our own population data (188 occurrences in total). Current-day bioclimatic data (MARSPEC; Sbrocco & Barber, 2013) were obtained at 5 minute resolution and models were generated

201 using cross-validation of ten replicate runs under the default MAXENT parameters. Model
202 performance was assessed based on the area under the receiver operating characteristic curve
203 (AUC). Models were projected onto reconstructed bioclimatic data for the LGM (ensemble
204 of five models: CNRM, ECBILTCLIO, FGOALS, HadCM and MIROC-322; Sbrocco,
205 2014).

RESULTS

GENETIC ANALYSES

No evidence of linkage disequilibrium was detected between any of the eight nuclear microsatellite loci analysed. Between six (Pelnoc_40622 and Pelnoc_44003) and 36 (Pelnoc_46263) alleles were detected, with a total of 136 (mean = 17 per locus). Within-population levels of observed (H_O) and expected (H_E) heterozygosity ranged from 0.426 (Rathlin Island) to 0.622 (Portofino; mean = 0.512) and from 0.554 (Rathlin Island) to 0.704 (Roscoff; mean = 0.636) respectively (Table 1). Levels of F_{IS} were significantly different from zero in twelve of the 14 populations, and ranged from 0.040 (Sole Bank) to 0.364 (Roscoff; mean = 0.193). Only two populations (Rathlin Island and Portofino) exhibited significant levels of relatedness between individuals ($r = 0.131$ and 0.136 respectively). Summary statistics by locus are given in Supplementary Table S1.

Mitochondrial COI sequences were obtained from 242 individuals. Two individuals were found to be heteroplasmic i.e. they displayed double peaks at multiple sites within the sequence, and were discarded from subsequent analyses. A total of 116 mitochondrial COI haplotypes were identified (Figure 2). These were structured into two groups (103 and 13 haplotypes respectively) separated by nine mutations. Only the most common haplotype was found in all 14 populations analysed, and 94 were found in a single individual. Within populations, between three (Galicia) and 19 (Villefranche-Sur-Mer) haplotypes were detected (mean = 12.21). Levels of haplotype (H) and nucleotide (π) diversity ranged from 0.700 (Galicia) to 0.979 (Sole Bank; mean = 0.904), and from 0.006 (North Atlantic and Dingle) to 0.015 (Malinbeg) respectively (Table 1). The divergence time between the two mtDNA groups was calculated as 1.529 MYA. The mismatch distribution analyses for the large (103 haplotypes) and small (13 haplotypes) clades indicated past population expansion (Figure

S1), as did the values for Tajima's D (large clade $D = -2.366$, $P < 0.01$; small clade $D = -1.783$, $P < 0.05$) and Fu and Li's F for the large clade ($F = -5.062$, $P < 0.05$), but not for the small clade ($F = -1.964$, NS).

The analysis of molecular variance (AMOVA) revealed a small but significant overall differentiation based on nuclear microsatellites ($\Phi_{ST[NUC]} = 0.025$; $P < 0.001$), but no significant structuring based on the mtDNA COI ($\Phi_{ST[MT]} = -0.01$; NS; Table 2). Likewise, the nuclear microsatellites indicated minimal but significant structuring between Atlantic and Mediterranean populations ($\Phi_{CT[NUC]} = 0.020$; $P < 0.001$), but no significant structuring based on the mtDNA COI ($\Phi_{CT[MT]} = -0.02$; NS; Table 2). Population-pairwise $\Phi_{ST[NUC]}$ values ranged from -0.021 (Shetland Islands / Armorica Shelf) to 0.081 (Armorica Shelf / Portofino), whilst pairwise $\Phi_{ST[MT]}$ values ranged from -0.074 (Bay of Biscay / Galicia) to 0.038 (Shetland Islands / Galicia). The BAPS analysis indicated that all the individuals analysed were grouped into a single genetic cluster (100% probability). This was reflected in the PCA, which showed no evidence of geographical structuring of individual multilocus genotypes (Figure 3).

The simulation studies suggested that the nuclear microsatellite data were able to detect F_{ST} values of as low as 0.005 at least 95% of the time (Figure 4). The mtDNA COI locus had much lower power, only 38% for $F_{ST} = 0.005$, and could only detect $F_{ST} > 0.018$ with a power of above 95%.

PALAEODISTRIBUTION MODELLING

For all models, AUC values were high (mean AUC = 0.908; SD = 0.040). The current-day model indicated the presence of suitable habitat for *P. noctiluca* along western Europe between 40 °N and 70 °N, including both the continental shelf and deeper waters off the Bay of Biscay / northwest Iberia and the Norwegian Sea (Figure 5a). The palaeodistribution

256 model indicated a southward shift in suitable habitat, with the maximum northern limit off
257 the palaeocoastline around 50 °N, as well as more extensive habitat in the Mediterranean Sea
258 (Figure 5b).

DISCUSSION

The findings of the present study based on high-resolution nuclear and mitochondrial markers indicate a high degree of connectivity in *Pelagia noctiluca* across the Northeast Atlantic and the Mediterranean. There was little overall evidence of geographical structuring of genetic variation, and only a small but significant differentiation of Atlantic Ocean and Mediterranean stocks based on the microsatellite data. No evidence of differentiation was observed with the mtDNA, reflecting the higher power of the microsatellites to detect low levels of genetic structuring as indicated by the POWSIM analysis (Larsson *et al.*, 2009). The observed high levels of genetic diversity across the entire range of the study, as well as the Atlantic-wide distribution of the species (Miller, von der Heyden & Gibbons, 2012) and, indeed, the pan-global distribution of what is at least a species complex (Kramp, 1961; Mariottini, Giacco & Pane, 2008), would appear to be inconsistent with the concept of a Gulf of Gibraltar source of recurring aggregations in the Northeast Atlantic Ocean and Western Mediterranean Sea as proposed previously by Licandro *et al.*, (2010).

Despite the lack of any geographical structuring of genetic variation, two clearly distinct groups of genotypes were observed within the mtDNA COI, a feature also observed by Stopar *et al.* (2010). Such divergences tend to result from periods of isolation, usually associated with the climatic fluctuations that have occurred throughout the Pleistocene (Provan & Bennett, 2008; Provan, 2013). The timing of the divergence, however, places it in the early Pleistocene (*ca.* 1.5 MYA), thus ruling out recent episodes of glaciation as the causal factor in promoting divergence. Furthermore, the palaeodistribution model suggests the persistence of a large, continuous population of *P. noctiluca* during the LGM, similar to the scenario observed in the zooplankton *Calanus finmarchicus* (Provan *et al.*, 2009), but in contrast to our earlier findings in the metagenic jellyfish *Rhizostoma octopus* (Glynn,

Houghton & Provan, 2015). The fact that individuals from both the Atlantic and the Mediterranean are represented by haplotypes from each clade, coupled with the observed lack of any structuring in the microsatellite data set, further suggests extensive admixture since the divergence of the two clades. If this mitochondrial structure were representative of contemporary, ongoing, sympatric divergence, a commensurate divergence in microsatellite lineages would be seen. As this is not the case, mitochondrial clades are likely vestigial remnants of allopatric divergence, subjected to subsequent secondary contact, range overlap and admixture. It is not obvious what factors would have promoted such a divergence *ca.* 1.5 MYA, but this period saw the start of a decrease in the North Atlantic Deep Water (NADW) formation, among a range of other oceanic and climatic changes at the same time, prior to the onset of the full glacial periods *ca.* 0.9 MYA (Raymo *et al.*, 1990; McClymont & Rosell-Melé, 2005). Phylogenetic divergence dating to around the same time period (*ca.* 1.2 – 1.8 MYA) has been reported for the fish species *Dentex dentex* and *Lithognathus mormyrus* (Bargelloni *et al.*, 2003), but in these cases this has resulted in separate Atlantic and Mediterranean clades.

Significant F_{IS} values were observed in all but two of the populations sampled, which could at first sight be attributed to intra-aggregation inbreeding, since it has been suggested previously that reproduction generally occurs within persistent aggregations of *P. noctiluca* (Russell, 1967; Zavodnik, 1987; Malej, 1989). This scenario, however, is not supported by the analyses of within-population relatedness. Furthermore, the high levels of genetic diversity observed across populations are inconsistent with long-term inbreeding. The Portofino population was one of the two that exhibited significant within-population relatedness between individuals, as well as being the most genetically distinct based on the nuclear pairwise Φ_{ST} estimates. This might be seen as evidence for intra-aggregation recruitment, but the same population did not exhibit a significant F_{IS} value. These apparent

309 discrepancies might be symptomatic of complex patterns of recruitment, including the
310 occurrence of Wahlund effects as a result of sampling distinct cohorts within a specific
311 geographical area that may have arisen through sweepstakes recruitment processes (Christie
312 *et al.*, 2010), but set against a long-term backdrop of high levels of broad-scale gene flow
313 over relatively long timescales. Nevertheless, the use of multiple, unlinked markers, and
314 particularly of markers which exhibit dissimilar mutation rates and patterns of inheritance in
315 the present study has proven useful in differentiating contemporary and historical signals of
316 population structure. Our findings point to the long-term persistence of a single, contiguous
317 European population of *P. noctiluca*, with minimal geographical structure. These results thus
318 provide key insights into the population dynamics and demography of this ecologically and
319 socio-economically important species.

ACKNOWLEDGEMENTS

We are grateful to Dave Stokes, the Marine Institute of Ireland, the Northern Ireland Environment Agency, Niall T. Keogh, Damien Haberlin, Lenaïg and Arzhela Hemery and others who provided samples, to Gemma Beatty for assistance in the laboratory, to Nils Ryman for advice on the POWSIM analyses, and to two anonymous Referees whose comments improved the manuscript. Fergal Glynn's PhD was funded by the Department of Agriculture and Rural Development, Northern Ireland (DARDNI). Martin Lilley was funded by l'Agence Nationale de la Recherche projects "Ecogely" ANR-10-PDOC-005-01 and "NanoDeconGels" ANR-12-EMMA-0008. He would also like to thank the Centre for Environment, Fisheries & Aquaculture Science for facilitating the collection of the Shetland samples.

REFERENCES

- Aglieri G, Papetti C, Zane L, Milisenda G, Boero F, Piraino S. 2014.** First evidence of inbreeding, relatedness and chaotic genetic patchiness in the holoplanktonic jellyfish *Pelagia noctiluca* (Scyphozoa, Cnidaria). *PLoS One* **9**: e99647.
- Arai MN. 1997.** *A Functional Biology of Scyphozoa*. Chapman & Hall, London, 316 pp.
- Bargelloni L, Alarcon JA, Alvarez MC, Penzo E, Magoulas A, Reis C, Patarnello T. 2003.** Discord in the family Sparidae (Teleosti): divergent phylogeographical patterns across the Atlantic-Mediterranean divide. *Journal of Evolutionary Biology* **16**: 1149-1158.
- Bastian T, Stokes D, Kelleher JE, Hays GC, Davenport J, Doyle TK. 2011.** Fisheries bycatch data provide insights into the distribution of the mauve stinger (*Pelagia noctiluca*) around Ireland. *ICES Journal of Marine Science* **68**: 436–443.
- Boero F, Bouillon J, Gravili C, Miglietta MP, Parsons T, Piraino S. 2008.** Gelatinous plankton: irregularities rule the world (sometimes). *Marine Ecology Progress Series* **356**: 299-310.
- Christie MR, Johnson DW, Stallings CD, Hixon MA. 2010.** Self-recruitment and sweepstakes reproduction amid extensive gene flow in a coral-reef fish. *Molecular Ecology* **19**: 1042-1057.
- Corander J, Waldmann P, Sillanpää MJ. 2003.** Bayesian analysis of genetic differentiation between populations. *Genetics* **163**: 367-374.
- Doyle TK, De Haas H, Cotton D, Dorschel B, Cummins V, Houghton JDR, Davenport J, Hays GC. 2008.** Widespread occurrence of the jellyfish *Pelagia noctiluca* in Irish coastal and shelf waters. *Journal of Plankton Research* **30**: 963–968.
- Doyle TK, Hays GC, Harrod C, Houghton JDR. 2014.** Ecological and societal benefits of jellyfish. In: Pitt KA, Lucas CH (Eds.), *Jellyfish Blooms* pp. 105–127. Dordrecht: Springer Netherlands.
- Excoffier L, Smouse PE, Quattro JM. 1992.** Analysis of molecular variance inferred from metric distances among DNA haplotypes - application to human mitochondrial DNA restriction data. *Genetics* **131**: 479-491.
- Excoffier L, Lischer HEL. 2010.** Arlequin suite ver 3.5: a new series of programs to perform population genetics analyses under Linux and Windows. *Molecular Ecology Resources* **10**: 564-567.

- Ferguson HW, Christian MJD, Hay S, Nicolson J, Sutherland D, Crumlish M. 2010.** Jellyfish as vectors of bacterial disease for farmed salmon (*Salmo salar*). *Journal of Veterinary Diagnostic Investigation* **22**: 376-382.
- Fleming NEC, Harrod C, Houghton JDR. 2013.** Identifying potentially harmful jellyfish blooms using shoreline surveys. *Aquaculture Environment Interactions* **4**: 263–272.
- Fraser JH. 1955.** The plankton of the waters approaching the British Isles in 1953. *Marine Research Scotland* **1**: 1-12.
- Glynn F, Houghton JDR, Provan J. 2015.** Population genetic analyses reveal distinct geographical blooms of the jellyfish *Rhizostoma octopus* (Scyphozoa). *Biological Journal of the Linnean Society* (In Press)
- Goudet J. 2002.** FSTAT, version 2.9.3, A program to estimate and test gene diversities and fixation indices. <http://www2.unil.ch/popgen/softwares/fstat.htm>.
- Govindarajan AF, Halanych KM, Cunningham CW. 2005.** Mitochondrial evolution and phylogeography in the hydrozoans *Obelia geniculata* (Cnidaria). *Marine Biology* **146**: 213-222.
- Houghton JDR, Doyle TK, Davenport J, Hays GC. 2006a.** Jellyfish aggregations and leatherback turtle foraging patterns in a temperate coastal environment. *Ecology* **87**: 1967-1972.
- Houghton JDR, Doyle TK, Davenport J, Hays GC. 2006b.** Developing a simple, rapid method for identifying and monitoring jellyfish aggregations from the air. *Marine Ecology Progress Series* **314**: 159-170.
- Kramp PL. 1961.** Synopsis of the medusa of the world. *Journal of the Marine Biological Association of the United Kingdom* **40**: 1-469.
- Larsson LC, Charlier J, Laikre L, Ryman N. 2009.** Statistical power for detecting genetic divergence – organelle versus nuclear markers. *Conservation Genetics* **10**: 1255-1264.
- Lee PLM, Dawson MN, Neill SP, Robins PE, Houghton JDR, Doyle TK, Hays GC. 2013.** Identification of genetically and oceanographically distinct blooms of jellyfish. *Journal of the Royal Society Interface* **10**: 20120920.
- Librado P, Rozas J. 2009.** DnaSP v5: a software for comprehensive analysis of DNA polymorphism data. *Bioinformatics* **25**: 1451-1452.
- Licandro P, Conway DVP, Daly Yahia MN, Fernandez de Puellas ML, Gasparini S, Hecq JH, Tranter P, Kirby RR. 2010.** A blooming jellyfish in the northeast Atlantic and Mediterranean. *Biology Letters* **6**: 688–91.

389 **McClymont EL, Rosell-Melé A. 2005.** Link between the onset of modern Walker circulation and the mid-
390 Pleistocene climate transition. *Geology* **33**: 389-392.

391 **Malej A. 1989.** Behaviour and trophic ecology of the jellyfish *Pelagia noctiluca* (Forsskål, 1775). *Journal of*
392 *Experimental Marine Biology and Ecology* **126**: 259-270.

393 **Mariottini GL, Giacco E, Pane L. 2008.** The mauve stinger *Pelagia noctiluca* (Forsskål, 1775). Distribution,
394 ecology, toxicity and epidemiology of stings. *Marine Drugs* **6**: 496-513.

395 **Miller BJ, vonder Heyden S, Gibbons MJ. 2012.** Significant population genetic structuring of the
396 holoplanktonic scyphozoan *Pelagia noctiluca* in the Atlantic Ocean. *African Journal of Marine Science*.
397 **34**: 425-430.

398 **Nei M, Kumar S. 2000.** *Molecular Evolution and Phylogenetics* Oxford University Press, Oxford.

399 **Patarnello T, Volckaert AMJ, Castilho R. 2007.** Pillars of Hercules: Is the Atlantic-Mediterranean transition
400 a phylogeographic break? *Molecular Ecology* **16**: 4426-4444.

401 **Pauly D, Graham WM, Libralato S, Morissette L, Deng Palomares ML. 2008.** Jellyfish in ecosystems,
402 online databases, and ecosystem models. *Hydrobiologia* **616**: 67–85.

403 **Peakall R, Smouse PE. 2006.** GENALEX 6 Genetic analysis in Excel. Population genetic software for research
404 and teaching. *Molecular Ecology Notes* **6**: 288-295.

405 **Phillips SJ, Anderson RP, Schapire RE. 2006.** Maximum entropy modeling of species geographic
406 distributions. *Ecological Modelling* **190**: 231-259.

407 **Porebski S, Bailey LG, Baum BR. 1997.** Modification of a CTAB DNA extraction protocol for plants
408 containing high polysaccharide and polyphenol contents. *Plant Molecular Biology Reporter* **15**: 8-15.

409 **Provan J, Bennett, KD. 2008.** Phylogeographic insights into cryptic glacial refugia. *Trends in Ecology and*
410 *Evolution*, **23**: 564-571.

411 **Provan J, Beatty GE, Keating SL, Maggs CA, Savidge G. 2009.** High dispersal potential has maintained
412 long-term population stability in the North Atlantic copepod *Calanus finmarchicus*. *Proceedings of the*
413 *Royal Society of London Series B – Biological Science* **276**: 301-307.

414 **Provan J. 2010.** Population genetics of microalgae. In: *Microbial Population Genetics* (ed. Xu JP), Caister
415 Academic Press, Norwich pp. 109-123.

416 **Provan J. 2013.** The effects of past, present and future climate change on range-wide genetic diversity in
417 Northern North Atlantic marine species. *Frontiers of Biogeography* **5**: 60-66.

418 **Purcell JE, Uye S, Lo WT. 2007.** Anthropogenic causes of jellyfish blooms and their direct consequences for
 419 humans: a review. *Marine Ecology Progress Series* **350**: 153-174.

420 **Purcell JE, Tilves U, Fuentes VL, Milisenda G, Olariaga A, Sabatés A. 2014.** Digestion times and
 421 predation potentials of *Pelagia noctiluca* eating fish larvae and copepods in the NW Mediterranean Sea.
 422 *Marine Ecology Progress Series* **510**: 201-213.

423 **Queller DC, Goodnight KF. 1989.** Estimating relatedness using genetic markers. *Evolution* **43**: 258-275.

424 **Raymo ME, Ruddiman WF, Shackleton NJ, Oppo DW. 1990.** Evolution of Atlantic-Pacific $\delta^{13}\text{C}$ gradients
 425 over the last 2.5 m.y. *Earth and Planetary Science Letters* **97**: 353-368.

426 **Rogers AR, Harpending H. 1992.** Population growth makes waves in the distribution of pairwise genetic
 427 differences. *Molecular Biology and Evolution* **9**: 552-569.

428 **Rottini Sandrini L, Avian M. 1983.** Reproduction of *Pelagia noctiluca* in the central and northern Adriatic
 429 Sea. *Hydrobiologia* **216**:197-202.

430 **Russell FS. 1967.** On the occurrence of the scyphomedusan *Pelagia noctiluca* in the English Channel in 1966.
 431 *Journal of the Marine Biological Association of the United Kingdom.* **47**: 363-366.

432 **Ryman N, Palm S. 2006.** POWSIM: a computer program for assessing statistical power when testing for
 433 genetic differentiation. *Molecular Ecology Notes* **6**: 600-602.

434 **Sabatés A, Pagès F, Atienza D, Fuentes V, Purcell JE, Gili J-P. 2010.** Planktonic cnidarians distribution and
 435 feeding of *Pelagia noctiluca* in the NW Mediterranean Sea. *Hydrobiologia* **645**: 153-165.

436 **Sbrocco EJ, Barber PH. 2013.** MARSPEC: ocean climate layers for marine spatial ecology. *Ecology* **94**:
 437 2013.

438 **Sbrocco EJ. 2014.** Palaeo-MARSPEC: gridded ocean climate layers for the mid-Holocene and Last Glacial
 439 Maximum. *Ecology* **95**: 1710.

440 **Smouse PE, Peakall R. 1999.** Spatial autocorrelation analysis of individual multiallele and multilocus genetic
 441 structure. *Heredity* **82**: 561-573.

442 **Stopar K, Ramšak A, Trontelj P, Malej A. 2010.** Lack of genetic structure in the jellyfish *Pelagia noctiluca*
 443 (Cnidaria: Scyphozoa: Semaestomae) across European seas. *Molecular Phylogenetics and Evolution* **57**:
 444 417-428.

445 **Weir BS, Cockerham CC. 1984.** Estimating F-statistics for the analysis of population structure. *Evolution* **38**:
 446 1358-1370.

- 447 **Wirth T, Bernatchez L. 2001.** Genetic evidence against panmixia in the European eel. *Nature* **409**: 1037-
448 1040.
- 449 **Zavodnik D. 1987.** Spatial aggregations of the swarming jellyfish *Pelagia noctiluca* (Scyphozoa). *Marine*
450 *Biology* **94**: 265-269.

Table 1. *Pelagia noctiluca* sampling locations and summary diversity statistics

Population	Latitude (N)	Longitude (W)	Nuclear					Mitochondrial			
			N	H_O	H_E	F_{IS}	r	N	h	H	π
Shetland Islands	60.457	0.973	24	0.540	0.647	0.172**	0.008 ^{NS}	22 [†]	17	0.965	0.009
Rathlin Island	55.290	6.197	22	0.426	0.554	0.235**	0.131***	24	14	0.833	0.008
North Atlantic	55.687	8.224	20	0.514	0.635	0.194**	0.035 ^{NS}	21	14	0.919	0.006
Malinbeg	54.664	8.785	23	0.537	0.647	0.173**	0.019 ^{NS}	23 [†]	14	0.913	0.015
Lehinch	52.934	9.350	23	0.455	0.615	0.266**	0.043 ^{NS}	22	16	0.948	0.011
Dingle	52.193	10.478	9	0.500	0.614	0.198**	0.012 ^{NS}	6	5	0.933	0.006
Sole Bank	48.750	8.167	23	0.591	0.615	0.040 ^{NS}	0.041 ^{NS}	20	17	0.979	0.011
Roscoff	48.727	3.983	15	0.455	0.704	0.364**	-0.091 ^{NS}	11	9	0.946	0.011
Armoricaian Shelf	46.879	4.749	16	0.519	0.662	0.222**	-0.011 ^{NS}	15	11	0.933	0.014
Bay of Biscay	46.446	2.552	9	0.540	0.648	0.177**	0.014 ^{NS}	6	4	0.800	0.012
Galicia	43.398	8.398	10	0.473	0.659	0.295**	-0.029 ^{NS}	5	3	0.700	0.013
Cadaques	42.286	-3.280	23	0.555	0.643	0.139**	0.025 ^{NS}	20	11	0.874	0.008
Villefranche-Sur-Mer	43.702	-7.324	24	0.439	0.648	0.249**	0.002 ^{NS}	24	19	0.960	0.011
Portofino	44.303	-9.211	24	0.622	0.608	-0.024 ^{NS}	0.136***	23	17	0.949	0.008

Abbreviations: N , number of individuals studied; H_O , observed heterozygosity; H_E , expected heterozygosity; F_{IS} , inbreeding coefficient; r , relatedness coefficient; h , number of haplotypes detected; H , gene diversity; π , nucleotide diversity. Significance of F_{IS} / r - * $P < 0.05$; ** $P < 0.01$ *** $P < 0.001$; NS – non-significant. [†] Includes one heteroplasmic individual (not analysed).

Table 2. Analysis of molecular variance (AMOVA)

Source of variation	Nuclear				Mitochondrial			
	d.f	Sum of squares	Variance	%	d.f	Sum of squares	Variance	%
Among populations (overall)	13	53.939	0.054	2.47***	13	5.877	-0.001	-0.11 ^{NS}
Within populations	516	1097.421	2.127	97.53	228	104.979	0.460	100.11
Atlantic vs Mediterranean	1	12.983	0.045	2.02***	1	0.379	-0.001	-0.18 ^{NS}
Among populations within regions	12	40.957	0.035	1.58***	12	5.497	-0.001	-0.03 ^{NS}
Within populations	516	1097.421	2.127	96.40***	228	104.979	0.460	100.21 ^{NS}

*** $P < 0.001$; NS – non-significant.

Table 3. Population-pairwise Φ_{ST} values. Lower diagonal matrix – nuclear; Upper diagonal matrix – mitochondrial. Values significantly different from zero are shown in bold.

SI	-	0.019	-0.003	0.000	0.014	-0.021	-0.002	-0.006	0.002	0.001	0.038	0.006	-0.011	0.002
RI	0.025	-	0.003	0.008	0.018	-0.036	0.030	0.000	0.008	-0.034	-0.035	-0.014	0.014	0.011
NA	0.011	0.019	-	-0.001	0.010	-0.022	0.006	-0.010	-0.002	-0.011	0.002	-0.001	-0.006	0.002
MA	0.002	0.038	0.007	-	0.005	-0.019	-0.007	-0.014	-0.005	0.003	0.021	0.000	-0.002	-0.015
LE	0.014	0.035	0.032	0.021	-	-0.010	-0.005	0.000	-0.024	-0.002	0.022	-0.007	-0.008	0.007
DI	0.025	0.051	0.033	0.030	-0.009	-	-0.009	-0.034	-0.024	-0.040	-0.026	-0.029	-0.027	-0.015
SB	-0.021	0.030	0.002	-0.018	-0.001	0.016	-	-0.009	-0.018	0.026	0.050	0.012	-0.009	-0.003
RO	-0.021	0.025	-0.001	-0.011	0.029	0.025	0.024	-	-0.013	-0.035	-0.001	-0.009	-0.011	-0.015
AS	-0.012	0.004	0.001	0.009	0.029	0.025	0.010	-0.001	-	-0.008	0.008	-0.011	-0.015	0.001
BB	-0.004	0.008	0.002	0.009	0.039	0.054	0.022	0.018	0.009	-	-0.074	-0.019	-0.002	0.008
GA	0.032	0.033	0.023	0.032	0.025	0.055	0.018	0.038	0.025	0.015	-	-0.013	0.025	0.027
CA	0.039	0.020	0.019	0.044	0.037	0.035	0.037	0.017	0.030	0.003	0.028	-	-0.003	-0.008
VM	0.019	0.013	0.008	0.022	0.026	0.021	0.005	0.003	0.014	-0.003	0.005	0.005	-	0.000
PO	0.074	0.071	0.074	0.071	0.052	0.065	0.068	0.062	0.081	0.052	0.041	0.024	0.039	-
	SI	RI	NA	MA	LE	DI	SB	RO	AS	BB	GA	CA	VM	PO

SI – Shetland Islands, RI – Rathlin Island, NA – North Atlantic, MA – Malinbeg, LE – Lehinch, DI – Dingle, SB – Sole Bank, RO – Roscoff,

AS – Armorica Shelf, BB – Bay of Biscay, GA – Galicia, CA – Cadaques, VM – Villefranche-Sur-Mer, PO – Portofino.

Figure Legends

Figure 1. Locations of sites sampled in this study.

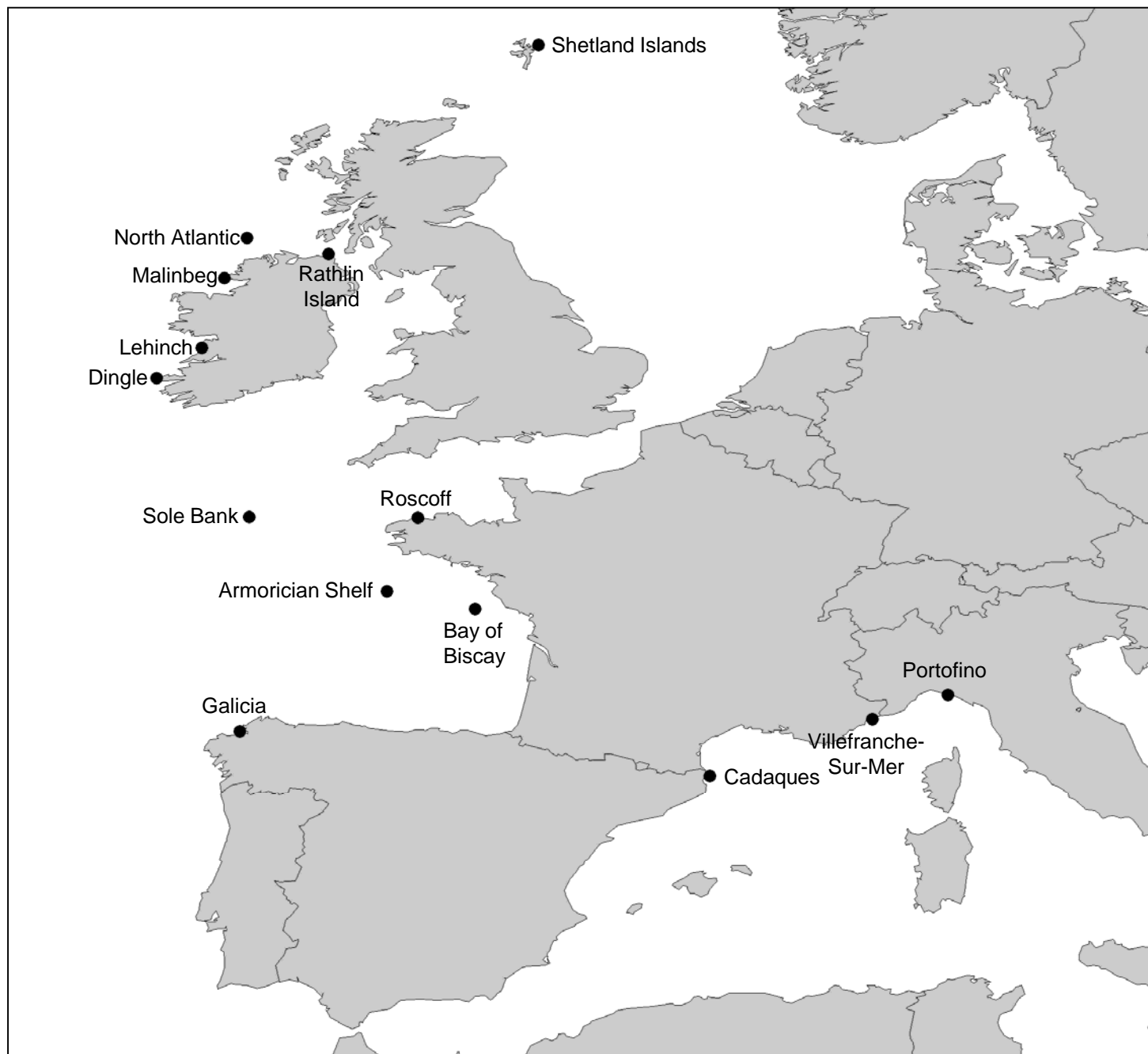
Figure 2. Median-joining network showing relationships between the 116 haplotypes detected by sequencing the mtDNA COI region. Circle sizes are approximately proportional to haplotype frequency: smallest circle represents a single individual, largest circle represents 66 individuals. Each connection represents a single mutation and small open diamonds represent missing intermediate haplotypes.

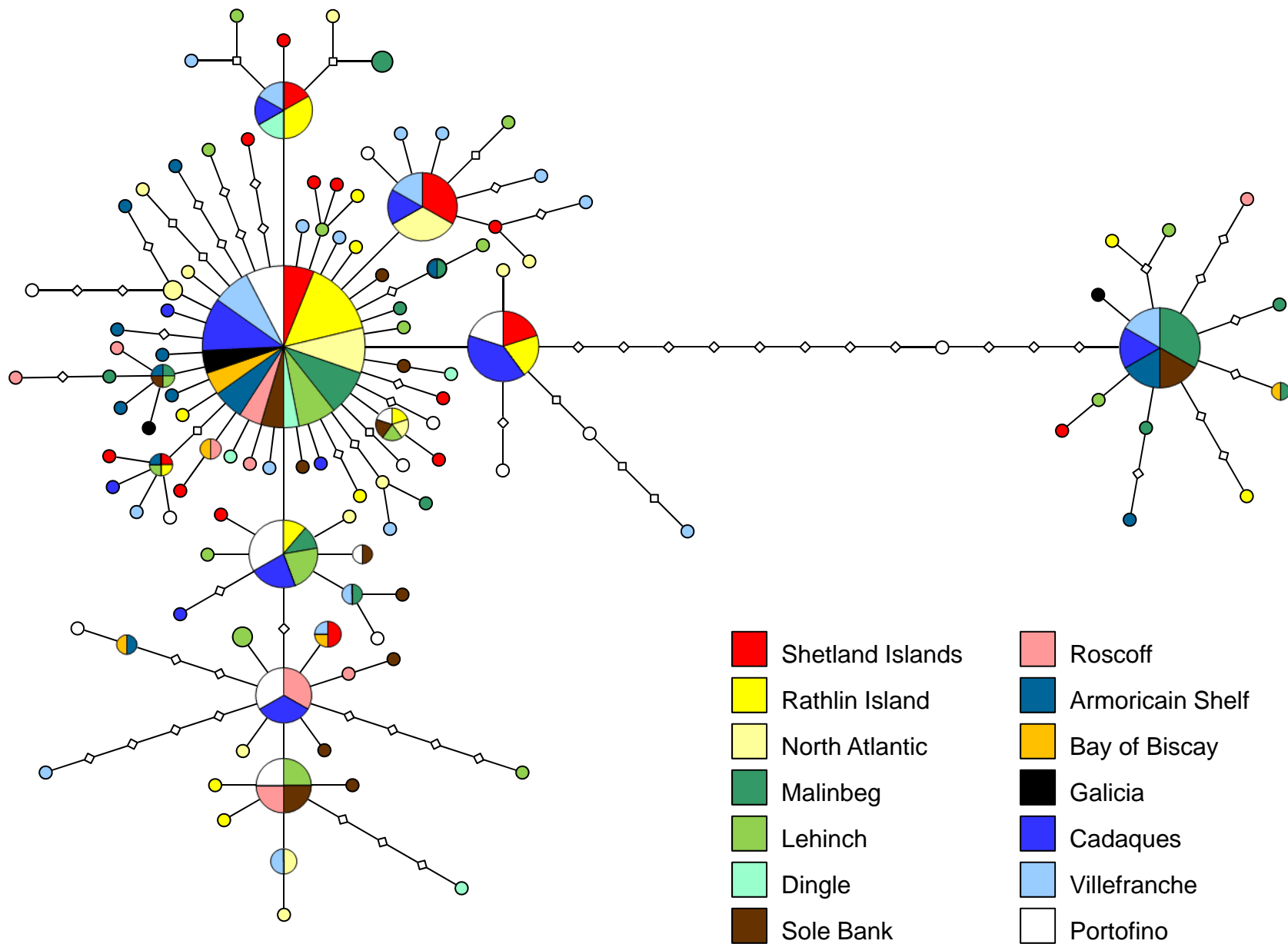
Figure 3. Results of the PCA. The first three axes accounted for 21.71%, 18.12% and 17.29% respectively of the total variation (57.13%).

Figure 4. Results of the POWSIM analysis. The Y-axis represents the power of the markers to successfully recover the value of F_{ST} indicated on the X-axis, expressed as the proportion of 1000 simulations (see text for details). For $F_{ST} = 0$, this is the Type I (α) value.

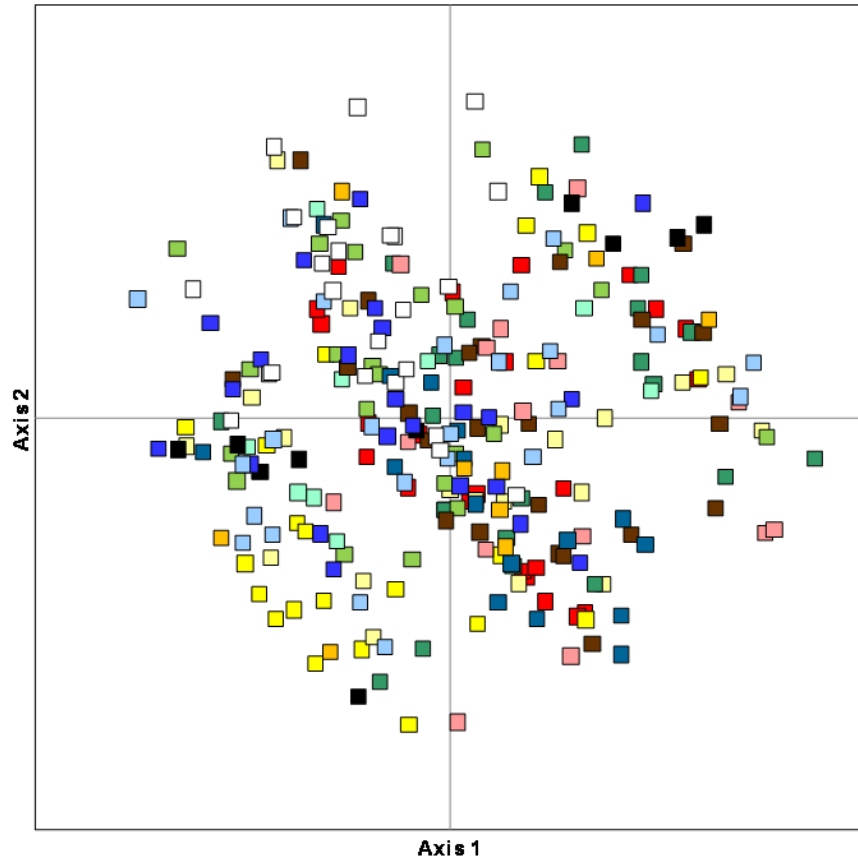
Figure 5. Results of the species distribution modelling: (a) current-day model; (b) palaeodistribution model for the Last Glacial Maximum (LGM *ca.* 21 KYA). Darker blue areas indicate those more suitable for *P. noctiluca*. Yellow circles in (a) indicate occurrence data used to generate the models.

Figure S1. Results of the mismatch distribution analyses.

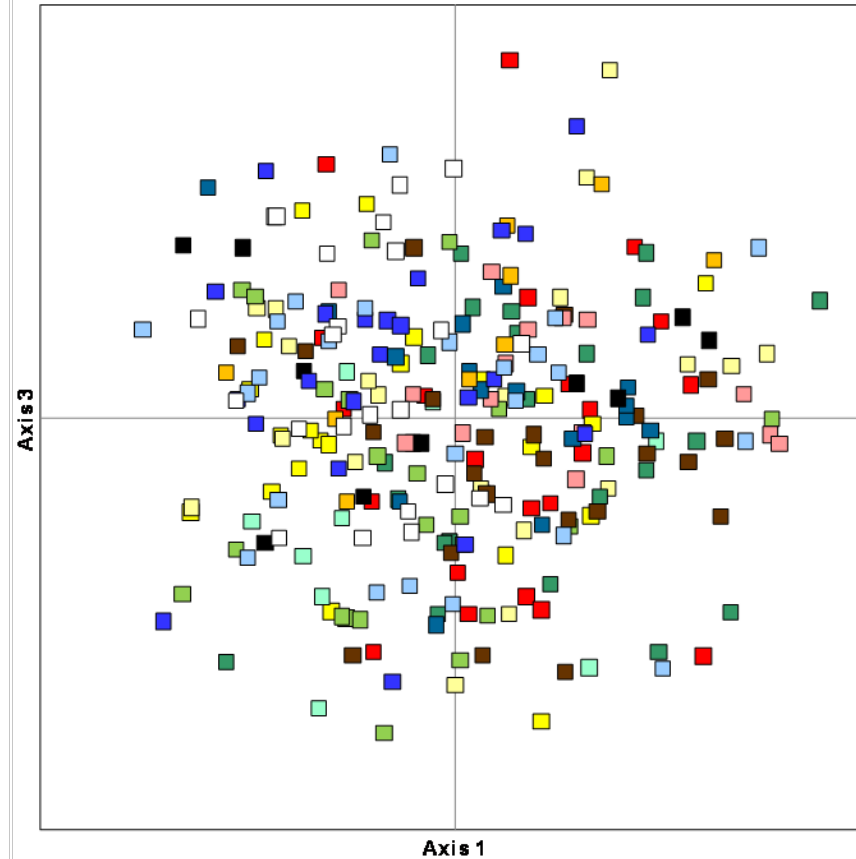




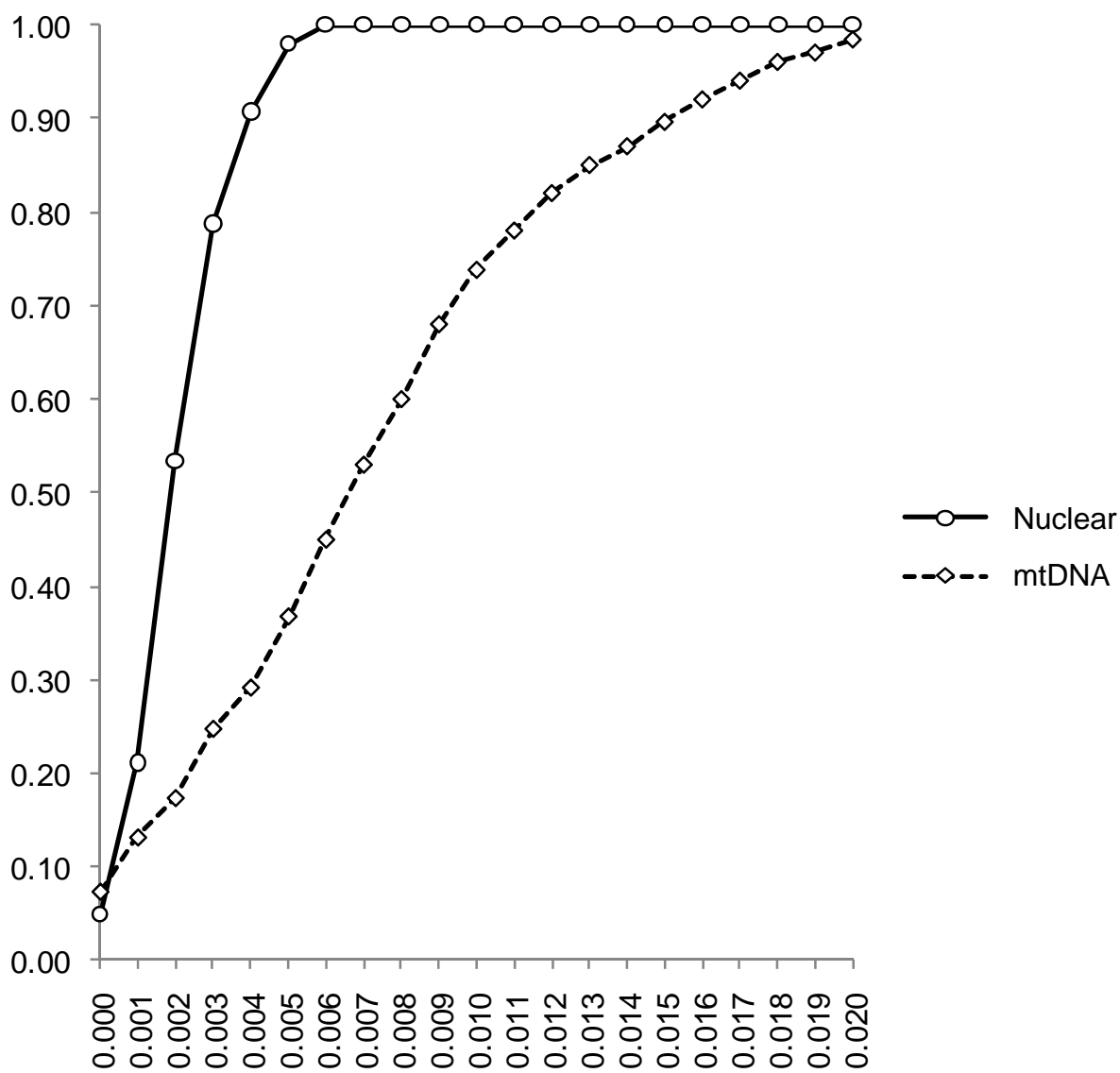
Principal Coordinates (1 vs 2)



Principal Coordinates (1 vs 3)



- Shetland Islands
- Rathlin Island
- North Atlantic
- Lehinch
- Malinbeg
- Dingle
- Sole Bank
- Roscoff
- Armoricaian Shelf
- Bay of Biscay
- Galicia
- Cadaques
- Villefranche-sur-Mer
- Portofino



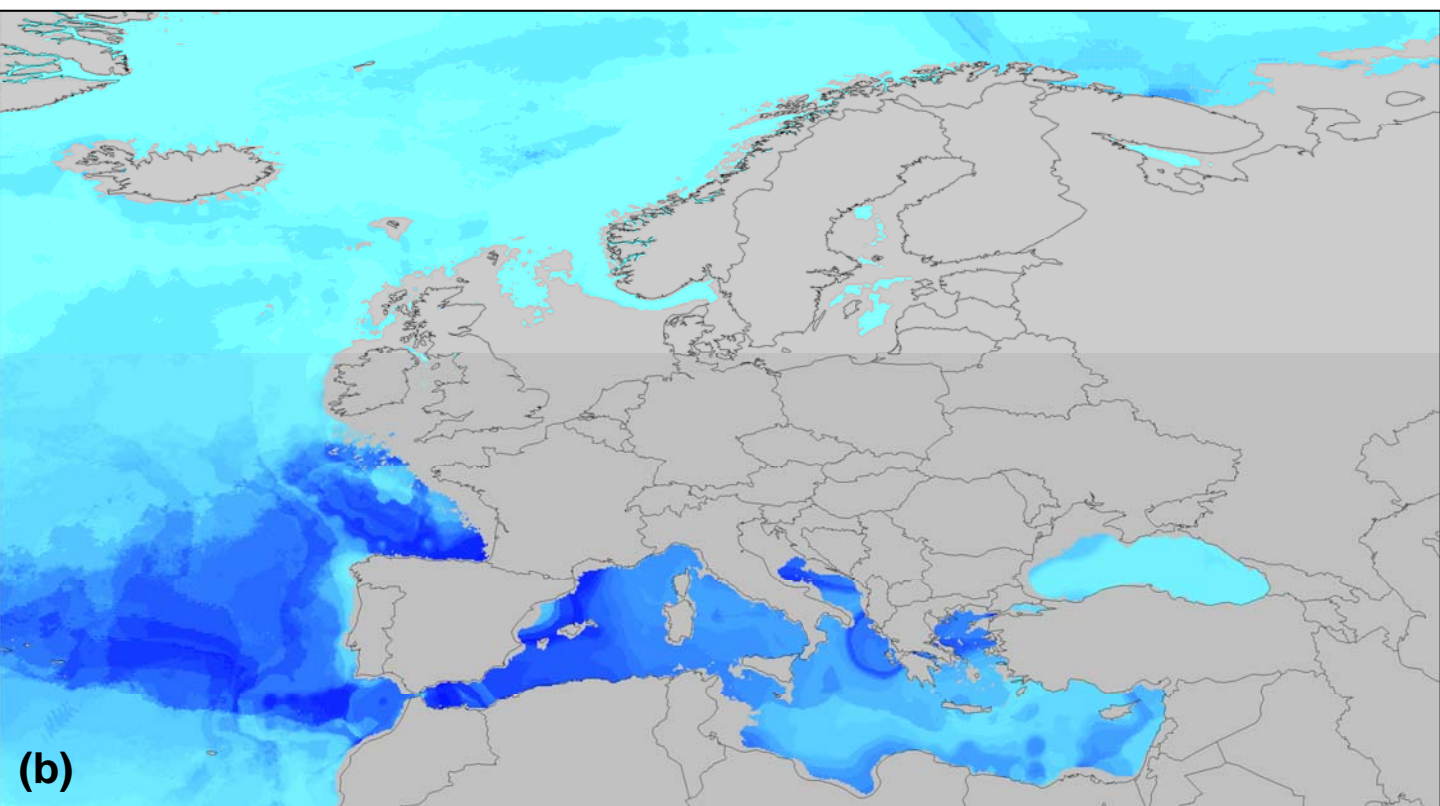
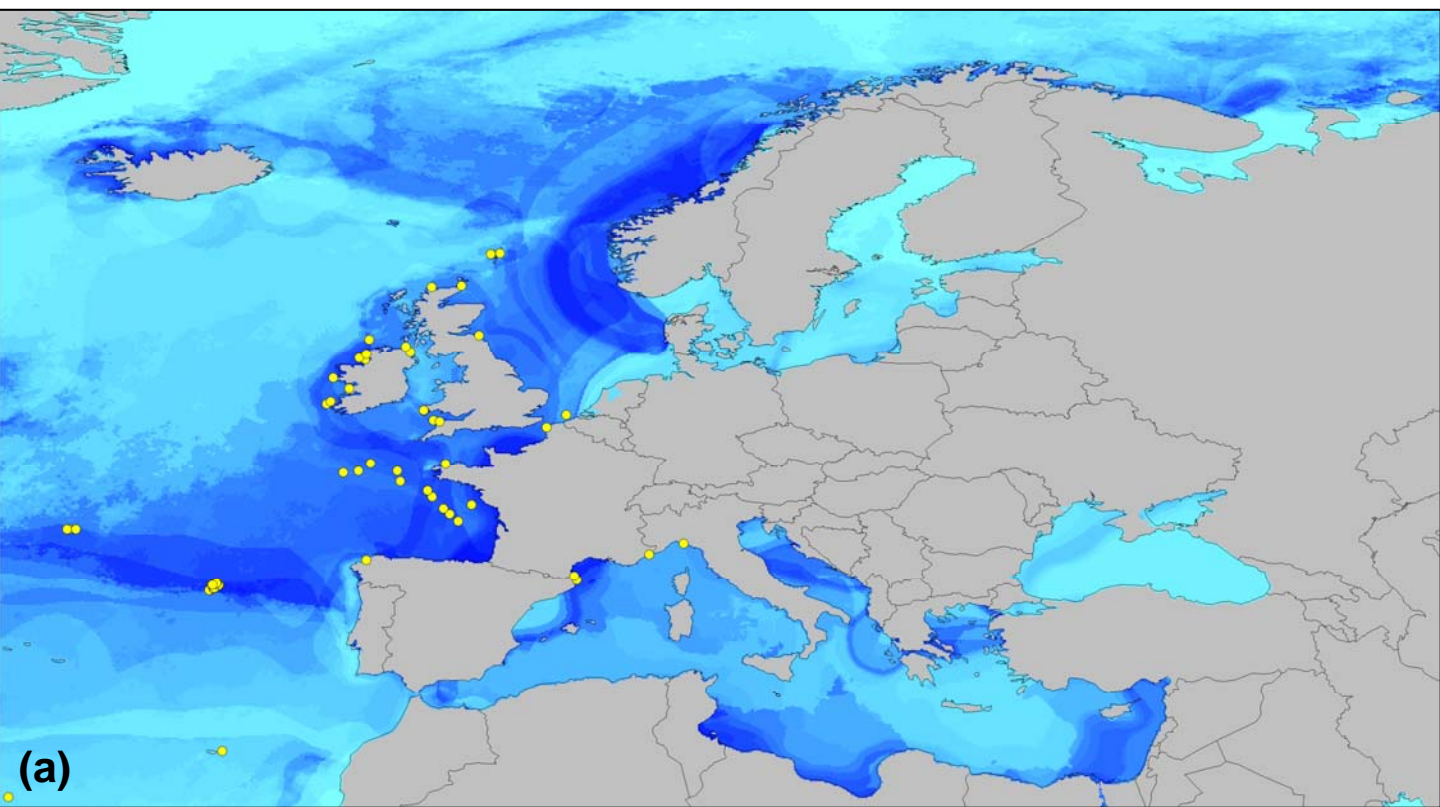
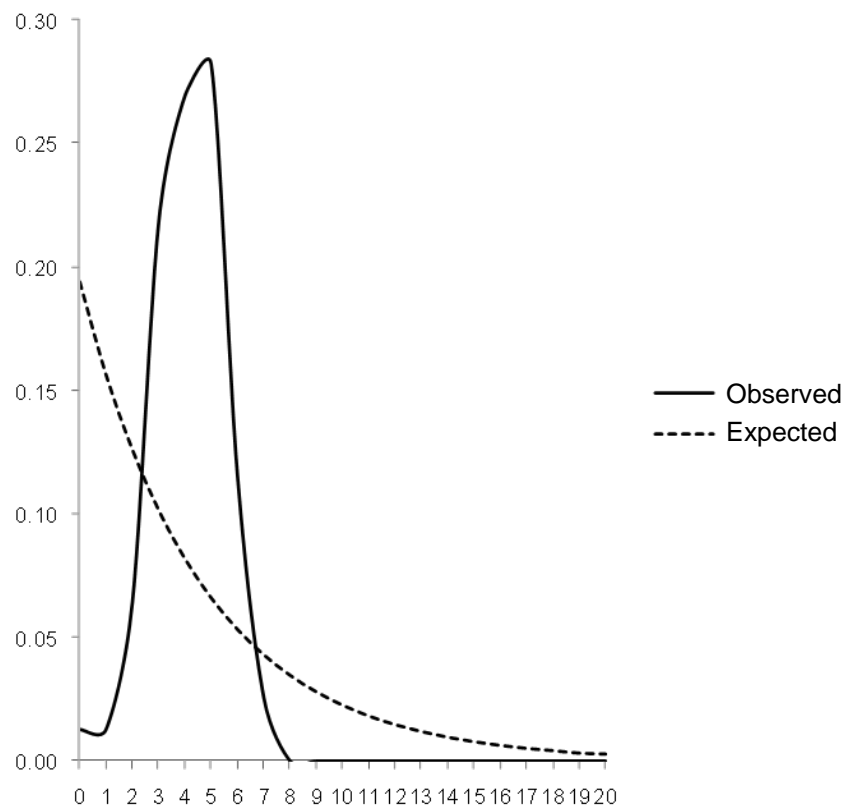
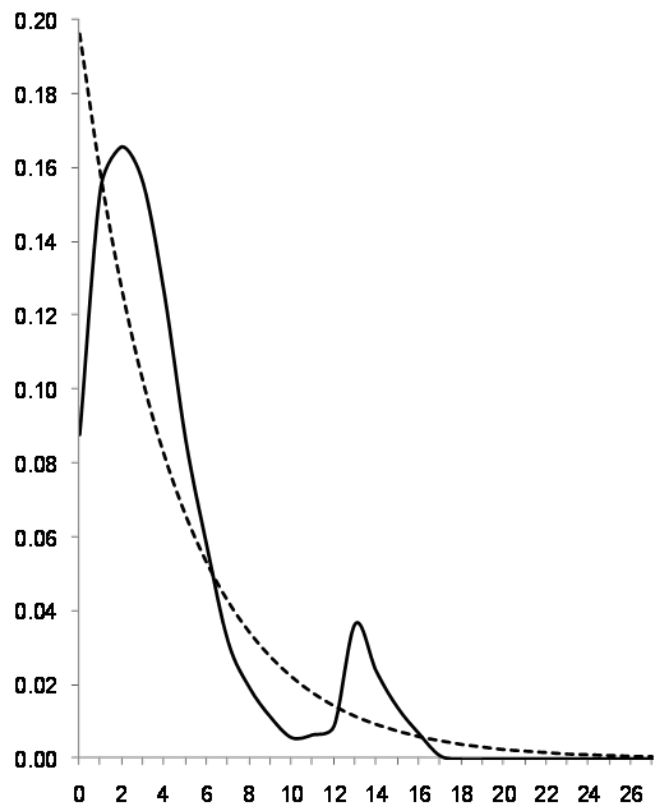


Table S1 Diversity statistics for each locus by population. Abbreviations: H_O , observed heterozygosity; H_E , expected heterozygosity; F_{IS} , inbreeding coefficient. Significance of F_{IS} - * $P < 0.05$; ** $P < 0.01$; NS – non-significant.

Population	Locus							
	Pelnoc_7445	Pelnoc_16756	Pelnoc_39456	Pelnoc_40428	Pelnoc_40622	Pelnoc_44003	Pelnoc_44210	Pelnoc_46263
Shetland Islands	$H_O = 0.435$	$H_O = 0.435$	$H_O = 0.500$	$H_O = 0.650$	$H_O = 0.375$	$H_O = 0.762$	$H_O = 0.522$	$H_O = 0.625$
	$H_E = 0.525$	$H_E = 0.622$	$H_E = 0.803$	$H_E = 0.635$	$H_E = 0.318$	$H_E = 0.540$	$H_E = 0.818$	$H_E = 0.917$
	$F_{IS} = 0.174^{NS}$	$F_{IS} = 0.306^*$	$F_{IS} = 0.383^{**}$	$F_{IS} = -0.025^{NS}$	$F_{IS} = -0.183^{NS}$	$F_{IS} = -0.425^{NS}$	$F_{IS} = 0.368^{**}$	$F_{IS} = 0.323^{**}$
Rathlin Island	$H_O = 0.500$	$H_O = 0.682$	$H_O = 0.474$	$H_O = 0.211$	$H_O = 0.045$	$H_O = 0.182$	$H_O = 0.600$	$H_O = 0.714$
	$H_E = 0.597$	$H_E = 0.594$	$H_E = 0.828$	$H_E = 0.201$	$H_E = 0.045$	$H_E = 0.444$	$H_E = 0.806$	$H_E = 0.914$
	$F_{IS} = 0.167^{NS}$	$F_{IS} = -0.152^{NS}$	$F_{IS} = 0.435^{**}$	$F_{IS} = -0.051^{NS}$	$F_{IS} = 0.000^{NS}$	$F_{IS} = 0.596^*$	$F_{IS} = 0.261^*$	$F_{IS} = 0.233^{**}$
North Atlantic	$H_O = 0.611$	$H_O = 0.600$	$H_O = 0.526$	$H_O = 0.500$	$H_O = 0.300$	$H_O = 0.526$	$H_O = 0.471$	$H_O = 0.579$
	$H_E = 0.668$	$H_E = 0.577$	$H_E = 0.717$	$H_E = 0.676$	$H_E = 0.276$	$H_E = 0.501$	$H_E = 0.768$	$H_E = 0.893$
	$F_{IS} = 0.088^{NS}$	$F_{IS} = -0.041^{NS}$	$F_{IS} = 0.271^{**}$	$F_{IS} = 0.266^*$	$F_{IS} = -0.091^{NS}$	$F_{IS} = -0.053^{NS}$	$F_{IS} = 0.395^{**}$	$F_{IS} = 0.358^{**}$
Malinbeg	$H_O = 0.714$	$H_O = 0.810$	$H_O = 0.261$	$H_O = 0.500$	$H_O = 0.391$	$H_O = 0.652$	$H_O = 0.286$	$H_O = 0.682$
	$H_E = 0.695$	$H_E = 0.771$	$H_E = 0.671$	$H_E = 0.553$	$H_E = 0.339$	$H_E = 0.585$	$H_E = 0.671$	$H_E = 0.890$
	$F_{IS} = -0.029^{NS}$	$F_{IS} = -0.051^{NS}$	$F_{IS} = 0.616^{**}$	$F_{IS} = 0.098^{NS}$	$F_{IS} = -0.158^{NS}$	$F_{IS} = -0.119^{NS}$	$F_{IS} = 0.580^{**}$	$F_{IS} = 0.238^{**}$
Lehinch	$H_O = 0.500$	$H_O = 0.476$	$H_O = 0.333$	$H_O = 0.500$	$H_O = 0.348$	$H_O = 0.455$	$H_O = 0.571$	$H_O = 0.455$
	$H_E = 0.686$	$H_E = 0.547$	$H_E = 0.716$	$H_E = 0.564$	$H_E = 0.294$	$H_E = 0.474$	$H_E = 0.747$	$H_E = 0.893$
	$F_{IS} = 0.276^{**}$	$F_{IS} = 0.132^{NS}$	$F_{IS} = 0.542^{**}$	$F_{IS} = 0.116^{NS}$	$F_{IS} = -0.189^{NS}$	$F_{IS} = 0.041^{NS}$	$F_{IS} = 0.239^*$	$F_{IS} = 0.497^{**}$
Dingle	$H_O = 0.556$	$H_O = 1.000$	$H_O = 0.375$	$H_O = 0.167$	$H_O = 0.667$	$H_O = 0.444$	$H_O = 0.125$	$H_O = 0.667$
	$H_E = 0.614$	$H_E = 0.775$	$H_E = 0.442$	$H_E = 0.439$	$H_E = 0.471$	$H_E = 0.601$	$H_E = 0.742$	$H_E = 0.830$
	$F_{IS} = 0.101^{NS}$	$F_{IS} = -0.318^{NS}$	$F_{IS} = 0.160^{NS}$	$F_{IS} = 0.643^{NS}$	$F_{IS} = -0.455^{NS}$	$F_{IS} = 0.273^{NS}$	$F_{IS} = 0.841^{**}$	$F_{IS} = 0.207^{NS}$
Sole Bank	$H_O = 0.609$	$H_O = 0.591$	$H_O = 0.600$	$H_O = 0.556$	$H_O = 0.435$	$H_O = 0.667$	$H_O = 0.632$	$H_O = 0.643$
	$H_E = 0.621$	$H_E = 0.557$	$H_E = 0.746$	$H_E = 0.513$	$H_E = 0.348$	$H_E = 0.512$	$H_E = 0.780$	$H_E = 0.844$
	$F_{IS} = 0.021^{NS}$	$F_{IS} = -0.062^{NS}$	$F_{IS} = 0.200^{NS}$	$F_{IS} = -0.086^{NS}$	$F_{IS} = -0.257^{NS}$	$F_{IS} = -0.311^{NS}$	$F_{IS} = 0.194^{NS}$	$F_{IS} = 0.245^*$
Roscoff	$H_O = 0.533$	$H_O = 0.429$	$H_O = 0.636$	$H_O = 0.286$	$H_O = 0.267$	$H_O = 0.333$	$H_O = 0.444$	$H_O = 0.714$
	$H_E = 0.687$	$H_E = 0.481$	$H_E = 0.861$	$H_E = 0.796$	$H_E = 0.441$	$H_E = 0.641$	$H_E = 0.824$	$H_E = 0.901$
	$F_{IS} = 0.230^{NS}$	$F_{IS} = 0.114^{NS}$	$F_{IS} = 0.271^{NS}$	$F_{IS} = 0.65^{**}$	$F_{IS} = 0.404^*$	$F_{IS} = 0.489^*$	$F_{IS} = 0.475^*$	$F_{IS} = 0.221^{NS}$

Table S1 (Continued)

Population	Locus							
	Pelnoc_7445	Pelnoc_16756	Pelnoc_39456	Pelnoc_40428	Pelnoc_40622	Pelnoc_44003	Pelnoc_44210	Pelnoc_46263
Armoricaian Shelf	$H_O = 0.563$	$H_O = 0.467$	$H_O = 0.462$	$H_O = 0.563$	$H_O = 0.231$	$H_O = 0.917$	$H_O = 0.500$	$H_O = 0.455$
	$H_E = 0.597$	$H_E = 0.563$	$H_E = 0.865$	$H_E = 0.728$	$H_E = 0.212$	$H_E = 0.554$	$H_E = 0.847$	$H_E = 0.926$
	$F_{IS} = 0.059^{NS}$	$F_{IS} = 0.176^{NS}$	$F_{IS} = 0.476^{**}$	$F_{IS} = 0.233^{NS}$	$F_{IS} = -0.091^{NS}$	$F_{IS} = -0.704^{NS}$	$F_{IS} = 0.419^{**}$	$F_{IS} = 0.522^{**}$
Bay of Biscay	$H_O = 0.625$	$H_O = 1.000$	$H_O = 0.556$	$H_O = 0.556$	$H_O = 0.222$	$H_O = 0.556$	$H_O = 0.375$	$H_O = 0.429$
	$H_E = 0.775$	$H_E = 0.659$	$H_E = 0.840$	$H_E = 0.569$	$H_E = 0.209$	$H_E = 0.529$	$H_E = 0.750$	$H_E = 0.846$
	$F_{IS} = 0.205^{NS}$	$F_{IS} = -0.585^{NS}$	$F_{IS} = 0.360^*$	$F_{IS} = 0.024^{NS}$	$F_{IS} = -0.067^{NS}$	$F_{IS} = -0.053^{NS}$	$F_{IS} = 0.517^*$	$F_{IS} = 0.514^*$
Galicia	$H_O = 0.500$	$H_O = 0.900$	$H_O = 0.778$	$H_O = 0.333$	$H_O = 0.200$	$H_O = 0.100$	$H_O = 0.222$	$H_O = 0.750$
	$H_E = 0.863$	$H_E = 0.679$	$H_E = 0.758$	$H_E = 0.562$	$H_E = 0.189$	$H_E = 0.521$	$H_E = 0.791$	$H_E = 0.908$
	$F_{IS} = 0.434^{**}$	$F_{IS} = -0.350^{NS}$	$F_{IS} = -0.028^{NS}$	$F_{IS} = 0.422^*$	$F_{IS} = -0.059^{NS}$	$F_{IS} = 0.816^*$	$F_{IS} = 0.731^{**}$	$F_{IS} = 0.184^{NS}$
Cadaques	$H_O = 0.591$	$H_O = 0.818$	$H_O = 0.611$	$H_O = 0.522$	$H_O = 0.182$	$H_O = 0.550$	$H_O = 0.500$	$H_O = 0.667$
	$H_E = 0.669$	$H_E = 0.643$	$H_E = 0.825$	$H_E = 0.647$	$H_E = 0.169$	$H_E = 0.514$	$H_E = 0.786$	$H_E = 0.887$
	$F_{IS} = 0.119^{NS}$	$F_{IS} = -0.281^{NS}$	$F_{IS} = 0.265^*$	$F_{IS} = 0.198^{NS}$	$F_{IS} = -0.077^{NS}$	$F_{IS} = -0.072^{NS}$	$F_{IS} = 0.370^{**}$	$F_{IS} = 0.253^{**}$
Villefranche-Sur-Mer	$H_O = 0.833$	$H_O = 0.625$	$H_O = 0.565$	$H_O = 0.417$	$H_O = 0.208$	$H_O = 0.458$	$H_O = 0.418$	$H_O = 0.391$
	$H_E = 0.793$	$H_E = 0.608$	$H_E = 0.823$	$H_E = 0.604$	$H_E = 0.191$	$H_E = 0.559$	$H_E = 0.832$	$H_E = 0.778$
	$F_{IS} = -0.051^{NS}$	$F_{IS} = -0.028^{NS}$	$F_{IS} = 0.318^{**}$	$F_{IS} = 0.314^{**}$	$F_{IS} = -0.095^{NS}$	$F_{IS} = 0.184^{NS}$	$F_{IS} = 0.504^{**}$	$F_{IS} = 0.503^{**}$
Portofino	$H_O = 0.545$	$H_O = 0.917$	$H_O = 0.700$	$H_O = 0.292$	$H_O = 0.250$	$H_O = 0.739$	$H_O = 0.818$	$H_O = 0.714$
	$H_E = 0.449$	$H_E = 0.598$	$H_E = 0.771$	$H_E = 0.571$	$H_E = 0.223$	$H_E = 0.530$	$H_E = 0.773$	$H_E = 0.948$
	$F_{IS} = -0.220^{NS}$	$F_{IS} = -0.552^{NS}$	$F_{IS} = 0.094^{NS}$	$F_{IS} = 0.495^{**}$	$F_{IS} = -0.122^{NS}$	$F_{IS} = -0.406^{NS}$	$F_{IS} = -0.060^{NS}$	$F_{IS} = 0.251^{**}$



— Observed
- - - Expected